EVALUATION OF HIGH DYNAMIC RANGE IMAGE BASED SKY MODELS IN LIGHTING SIMULATION

Mehlika Inanici
University of Washington, Department of Architecture, Box 355720, Seattle, WA, 98195.
inanici@uw.edu

1. INTRODUCTION

The accuracy of lighting simulations depends on the physically based modeling of the building and site properties, as well as the algorithmic reliability of the computational tools. Despite many developments in lighting simulation in the past decades, faithful representation of the sky luminance distributions at a specific location and time continues to be a challenge.

Daylight availability and sky luminance distributions vary spatially and temporally depending on geography, weather, and other local conditions. Substantial amount of data is accumulated from long term measurements in various parts of the world (Kitler et al. 1992) through sky scanners. These devices (such as the Krochmann sky scanner) typically measure luminance at 145 points. The accumulated data is used to establish generic predictive sky models in the form of mathematical formulae. Currently, International Commission on Illumination (CIE) has identified 15 generic sky models that cover conditions varying from overcast to cloudless skies (CIE 2003). Lighting simulation software utilize standard sky models (most commonly available models are the CIE overcast sky, clear sky and intermediate sky). However, these generic models do not represent actual sky conditions specific for any location; thus create high levels of uncertainty in the simulation and software validation processes. Moreover, due to the limited number of measurement points, the generic models do not have enough resolutions to adequately represent luminance variations, such as the rapid changes around the boundaries of clouds in an actual sky. The CIE sky models do not also include the spectral variations in the sky dome (Chain et al. 2001, Navvab 2005). These shortcomings hinder the predictive power and the fidelity of the simulation results. Therefore, there is a need for the development of sky models that encompass high resolution data to acquire the spatial variability within the sky dome.

Previously, a number of researchers have utilized photography to derive empirical sky models (Shahriar et al. 2009, Spasojevic and Mahdavi 2007, Uetani et al. 1993). The common approach in these studies is to capture the sky through a single photograph using a calibrated camera. The manual calibration process is tedious and camera dependent. Moreover, single image approach provides a limited dynamic range of luminance values. The acquired photograph is used to derive a customized mathematic model, and it is not used as a direct simulation input.

The technique utilized in this paper draws from developments in the field of Computer Graphics: High Dynamic Range (HDR) Photography and Image Based Lighting (IBL). In HDR Photography, multiple exposure photographs are taken to capture the wide luminance variation within a scene (Debevec and Malik 1997; Reinhard et al. 2006). The camera response function is computationally derived through a self calibration algorithm; and then it is used to fuse these photographs into a single HDR image, where pixel values can correspond to the physical quantity of luminance.

IBL is a visualization technique that utilizes captured HDR images as light sources in the rendering process (Debevec 2002). This paper demonstrates the use of 180° HDR images of the sky dome in lieu of the CIE sky models. Actual sky conditions at a place and time are captured through HDR photography technique. The luminance information stored at a pixel level is used to light the simulated environment. IBL is not specifically developed for lighting simulation purposes. Although few applications have been developed for architectural visualizations (Torres 2003; Debevec 2005; de Valpine 2006), there is a need for a comprehensive evaluation to determine the appropriateness of the technique for lighting simulation.

The goal of this research is to develop advanced lighting simulation techniques to empower researchers and practitioners with better predictive capabilities. The specific objectives include (i) development and utilization of high resolution data acquisition techniques to collect image based sky luminance information; (ii) demonstration of the utilization of the image based sky models in lighting simulations; and (iii) evaluation of image based sky models.

2. METHODOLOGY

The research consists of 4 main steps:

- HDR images of the sky dome are captured at different times and under different sky conditions.
- Simultaneously, HDR images of a daylit office interior are captured to measure the luminance properties of the office under current sky conditions.
- Physically based Rendering (PBR) and IBL techniques are used to simulate the same office with CIE sky models and captured sky images.
- Captured and simulated lighting conditions are compared. Uncertainties in the simulation, accuracy, expected errors, applicability, limitations, and advantages of the techniques are discussed.

2.1 HIGH DYNAMIC RANGE PHOTOGRAPHY

Capturing a luminous environment with HDR photography is a straightforward task. Multiple exposure photographs of static scenes can be taken with a commercially available digital camera to capture the wide luminance variation within the scenes. The camera response function is computationally derived, and then used to fuse the multiple photographs into an HDR image. This approach has been validated for lighting measurement purposes (Inanici and Galvin 2005, Inanici 2006). Laboratory and field studies show that the pixel values in the HDR photographs can correspond to the physical quantity of luminance with reasonable precision and repeatability (within 10% error margin).

HDR images of the sky dome are captured on the roof of the Architecture Hall at the University of Washington in Seattle during a period between December and July. Simultaneously, HDR images of a west facing office interior are captured in the second floor of the same building.

Sky images are captured with a commercially available digital camera (Canon EOS 5D) and fisheye lens (Sigma 8mm F3.5 EXDG that has 180° angle of view and equi-angle projection properties) that is mounted on a tripod. Multiple exposure photographs are captured while keeping white balance and ISO settings constant (daylight and 100, respectively) in order to achieve consistent color space transitions.

As a general rule, it is recommended to fix the aperture size and vary only the shutter speed (Inanici 2006). Under cloudy sky conditions, sky images are taken with a fixed aperture size (f/5.6), and varying the shutter speed in manual exposure mode (Fig. 1). The number of captured images varies based on the luminance breadth to be recorded. In general, 10 or more images are captured as the shutter speeds varied between 15 and 1/8000 seconds, using the three-stop increments. The shutter speed range is usually shortened under heavily cloudy skies, such that the longest exposure is not all washed out and the shortest exposure is not all black (Ward, 2005).

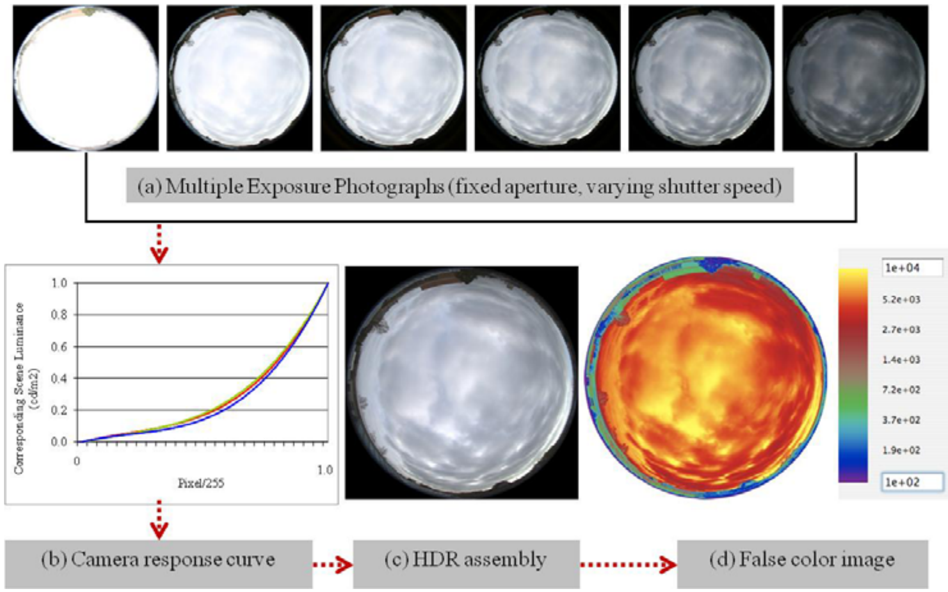

Fig. 1. Multiple exposure photographs taken with a fixed aperture size (f/5.6) and varying shutter speeds (a), assembled using the camera response curve (c), false color images (d) reveal the luminance distribution patterns

When the solar corona is visible, it is not possible to record the extreme dynamic range only using a fixed aperture size. To capture both the sky and the sun, the capturing process was modified to include two different apertures (f/4.0 and f/16) with varying shutter speeds as well as a neutral density filter (Kodak Wratten 2 Optical Filter), as demonstrated by Stumpfel et al. (2004). The number of captured images again varies based on the luminance breadth to be recorded. In general, 10 or more images are captured with the f/4 aperture size as the shutter speeds varies between 15 and 1/30 seconds, and with the f/16 aperture as the shutter speed varies between 1/15 and 1/8000 seconds (Fig. 2). This approach allows recording the extreme values in the sky dome under intermediate and clear skies (22-stop range corresponds to 7 logarithmic units).

Each multiple exposure sequence is fused into an HDR image using software called Photosphere (Ward, 2005). The assembly process succeeds the calculation of the camera response functions of the camera, which was performed automatically through a built-in self calibration algorithm within the software.

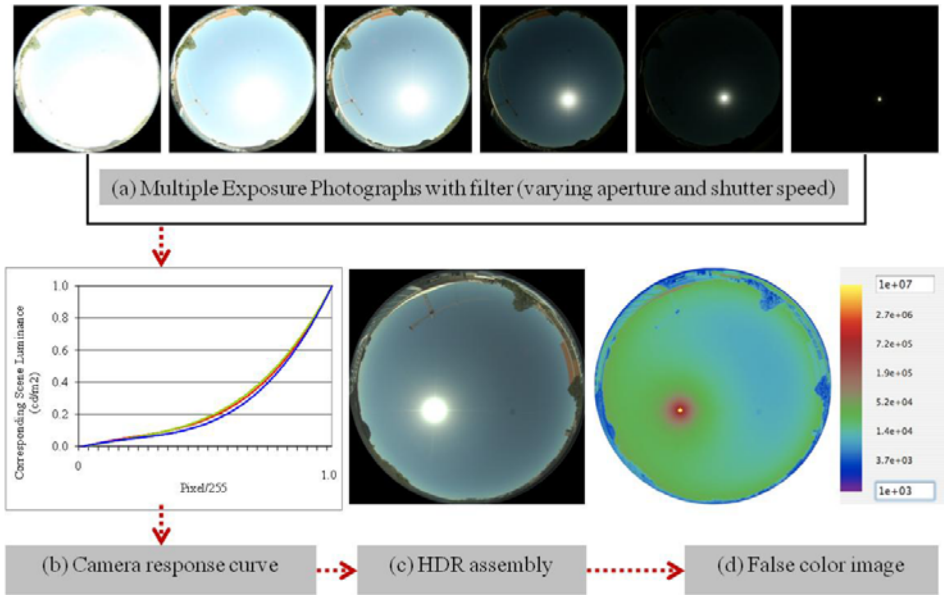

Fig. 2. Multiple exposure photographs taken with two aperture sizes (f/4 and f/16) and varying shutter speeds

Fisheye lenses exhibit noticeable vignetting, i.e. light fall off for the pixels far from the optical axis. Although vignetting effects are negligible in the center of the image, there are increasing errors towards the peripheral pixels. The vignetting effect of the fisheye lens is strongly dependent on the aperture size. This discrepancy is significant in capturing the sky luminance. Vignetting is determined through laboratory measurements done in 5° intervals for the three aperture sizes used in capturing the sky images (f/4.0, f/5.6, and f/16). The resulting light fall off is a different polynomial function for each of these aperture sizes. These functions are used to devise digital filters to compensate for the luminance loss (Fig. 3). The digital filter is an image that has the same resolution as the fisheye image, and it is applied as a post process to compensate for the vignetting effect based on the pixel location. For the image sequences that have two aperture sizes, partial HDR images are computed for each aperture size. As seen from Fig. 3, the vignetting effect for aperture f/4 is much more than the aperture f/16. The partial images are combined after the vignetting effect is compensated based on the corresponding aperture size.

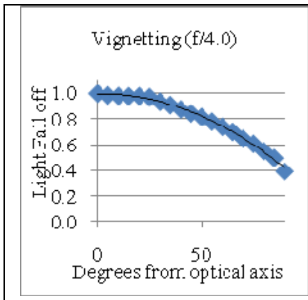

y = -7E-05x2 + 0.0003x + 0.9932

R² = 0.997

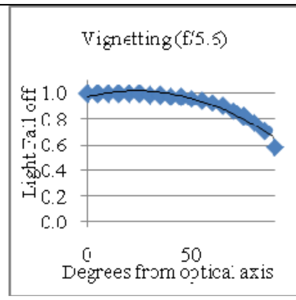

$y = -2E\text{-}08x^4 + 3E\text{-}06x^3 - 0.0001x^2 + 0.0021x + 0.9955$, $R^2 = 0.9975$

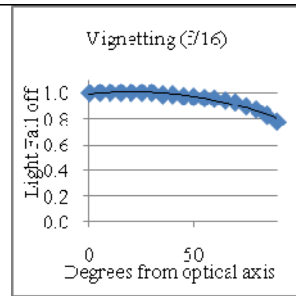

$y = -4E\text{-}05x^2 + 0.0017x + 0.991$

$R^2 = 0.9678$

Normalized luminance values

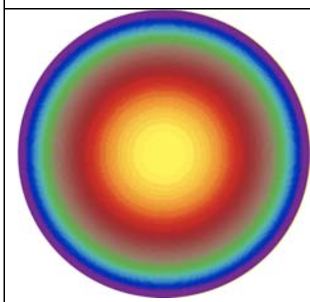

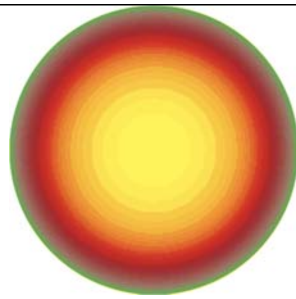

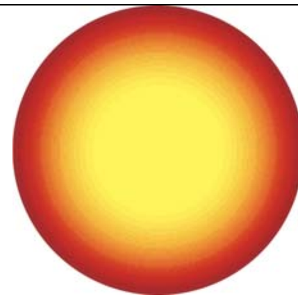

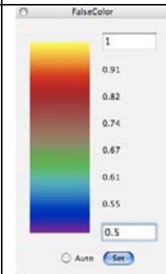

Fig. 3. Vignetting function of the fisheye lens is determined as the camera is rotated in 5° intervals away from the target, the camera response function for each aperture is determined as a polynomial fit (top row), and used to create a digital filter (bottom row) that is applied as a post process to compensate for the light fall off.

Although the luminance values in HDR images are calculated using the polynomial self calibration algorithm (shown in Fig. 1 and 2), it is recommended to linearly fine-tune the results with a single measurement (Inanici 2006). This linear calibration is especially essential with image sequences that incorporate the neutral density filter (Kodak Wratten 2 Optical Filter). Luminance values are calculated in cd/m^2 from the pixel values in HDR images. In general, a single luminance value of a gray target is measured (using a Minolta LS110 luminance meter) from the camera viewpoint during image capturing process and the calibration feature of Photosphere is used for fine tuning the luminance values within each image. However, this is not a practical approach to calibrate sky images. Instead, horizontal illuminance is measured at the camera level (using a Minolta T-10 illuminance meter) during the image capturing process of the sky dome. Illuminance can be derived from the average luminance values in hemispherical fisheye images. Hemispherical fisheye projection is a half sphere projected such that each differential area corresponds to the original area multiplied by the cosine of the polar angle (Ward and Shakespeare 1997). Therefore, it precisely compensates for the cosine correction. As a result, illuminance value can be derived from luminance values in a hemispherical fisheye projection as shown in Fig. 4.

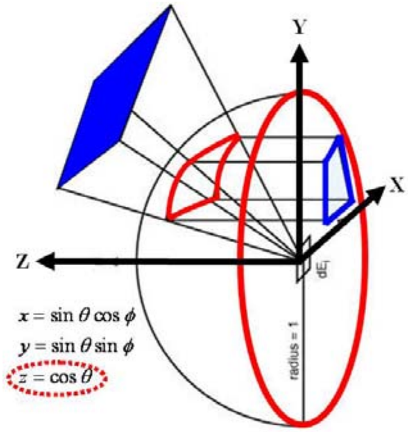

E = Illuminance
L (θ,ϕ): Luminance in the direction of θ,ϕ.

For any hemisphere of luminance L(θ,ϕ), the horizontal illuminance E is calculated as:

$$E = \int_0^{2\pi}\int_0^{\pi/2} L(\theta,\phi)\sin\theta\cos\theta d\theta d\phi \qquad (1)$$

For a uniform luminance $L(\theta,\phi) = L$

$$E = \pi L \qquad (2)$$

Fig. 4. Calculation of illuminance from luminance values in a hemispherical fisheye projection

Currently available fisheye lenses exhibit equi-distant projection. This projection is transformed into hemispherical fisheye projection for illuminance calculation purposes (Fig. 5) to calculate the iluminance value. Then, the horizontal illuminance measurement done at the camera level (using a Minolta T-10 illuminance meter) during the image capturing process of the sky dome is used to linearly calibrate the pixel values.

Images taken with and without neutral density filter in laboratory conditions revealed that neutral density filter shifts colors. Macbeth color chart was photographed and the color shift was particularly evident for the blue channel. The color aberration can be corrected by photographing a Macbeth chart under prevailing light conditions; a linear transformation function can be computed from the measured color space into the standard color space.

Interior photographs are captured with a Canon EOS 30D camera and Canon EF 20mm f/2.8 lens. Each multiple exposure sequence is fused into an HDR image using Photosphere. The assembly process succeeds the self calibration process that automatically determines the camera response functions. Each image is linearly fine tuned with a single luminance value of a gray target that is measured from the camera viewpoint during the image capturing process using a luminance meter (Minolta LS110).

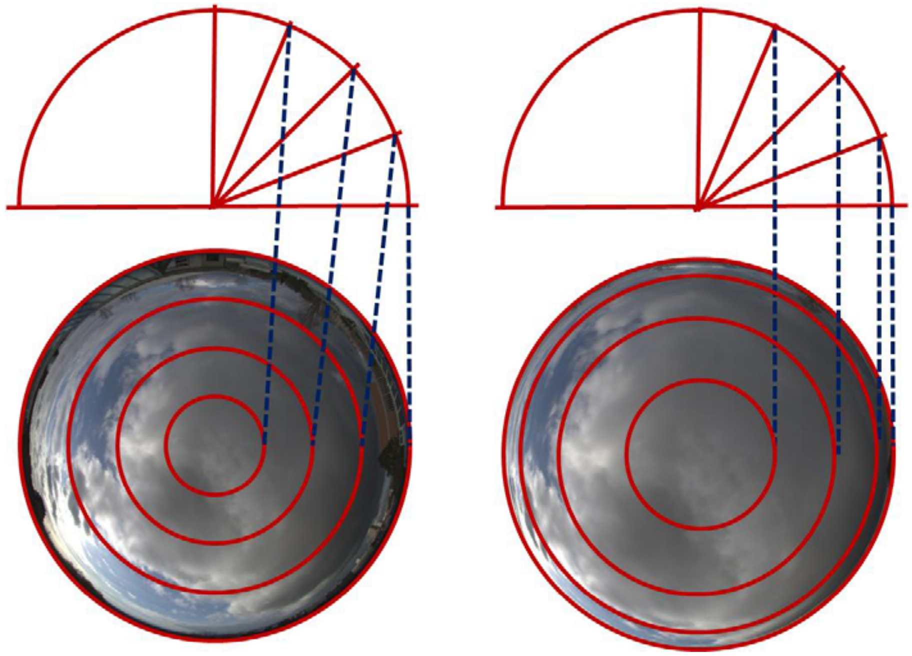

Fig. 5. Equi-distant (left) fisheye image of the sky is transformed into hemispherical fisheye projection (right): a hemispherical fisheye image demonstrates the volume seen by the illuminance meter as measurements are taken.

2.2 SIMULATION

Radiance Lighting Simulation and Visualization system (Ward, 1994) is used to simulate the office space both with the CIE skies and captured images. IBL technique was also originally developed using the Radiance software (Debevec, 2002).

It is necessary to create accurate (i.e. physically based) modeling of the environment for performing a real-world lighting analysis. Dimensions of the office space are measured on site (2.6m x 4.4m x 4.5m) and a 3D model is created (Fig. 6). The color and reflectance of materials are measured using Minolta CM-2002 Spectrophotometer. Some of the measured diffuse and specular reflectance values are as follows: concrete wall (29%, 0%), plaster wall (62%, 0.77%), ceiling tiles (75%, 0%), floor (15%, 1.43%), desktop (17%, 1.68%). Double glazed window is west facing. Glass properties are obtained from the manufacturer (73% visible light transmission).

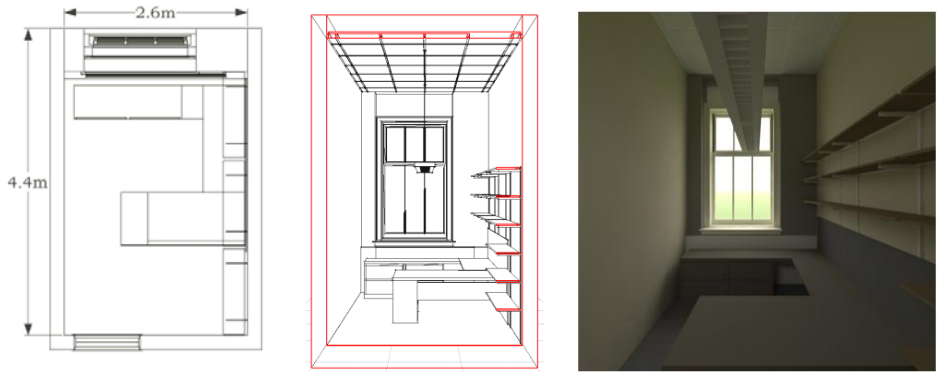

Fig. 6. Plan of the office, 3D model, and an interior view

In a Physically Based Rendering (PBR) system, daylight availability is defined through a sun description (distant light source) and a sky model (skylight). Direction and intensity of sunlight is calculated based on latitude, longitude, date, and time. The sky geometry is defined through an invisible hemisphere. Luminance distribution patterns over the hemisphere (i.e. sky dome) are calculated based on latitude, longitude, CIE sky type, and turbidity.

In an IBL system, the fisheye image of the sky dome is used in place of the mathematical definitions of the sun and the sky. A fisheye image of the sky is a parallel projection of the sky dome onto a circle, and therefore, the circle (fisheye image) can be projected back onto a hemisphere (Fig. 7). For the rendering process, the mathematical model of the sun and the CIE sky are removed from the simulation input; and the HDR image of the sky dome is included in form of an invisible, light emitting hemisphere. Pixel values in the HDR image correspond to the physical quantity of luminance (cd/m^2), therefore, each pixel 'glows' with its luminance value providing a source of illumination. Individually, each pixel represents the luminous intensity in a given direction per unit area; direction is determined by the position of the pixel (patch) in the sky dome. Collectively, pixels form the entire sky dome (sunlight and skylight) that provide real world lighting conditions, under which any built/natural environment can be simulated.

3. EVALUATION AND DISCUSSION

Evaluation of the IBR technique with image based sky models are done in two categories: The first category is a theoretical validation, where the objective is to study the accurateness of the IBL technique in comparison to PBR. The second category includes the empirical evaluation of the IBL technique, where the objective is to compare the IBL results with real world measurements.

3.1 THEORETICAL VALIDATION

For the theoretical validation, the interior office space is first simulated under standard CIE skies for Seattle, 47.6° North 122.3° West (refereed as the 'PBR technique'). Then, a fisheye image of the sky dome is simulated for the same time and location. Theoretically, if a standard CIE sky was occurring and captured using an HDR photograph, this photograph would be identical with the image of the sky generated within the Radiance program.

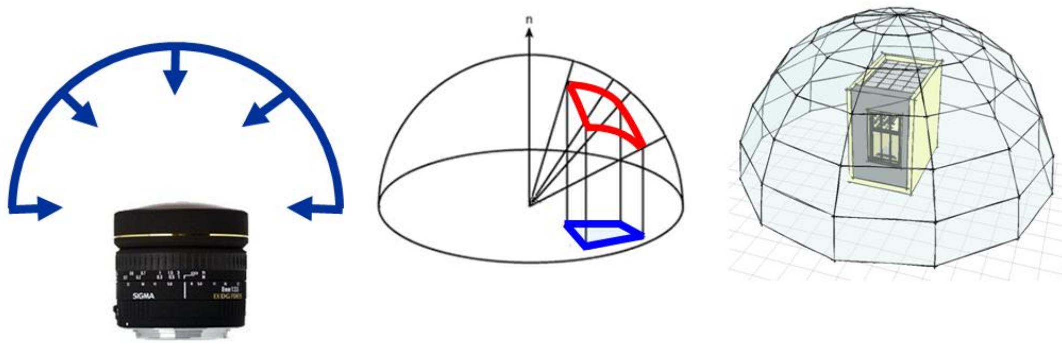

Fig. 7. Fisheye projections and application of a fisheye image as a light emitting hemisphere

Both HDR photographs and physically based renderings saved in HDR image format (i.e. .hdr) allow us to collect and generate visual and numerical lighting information in i) high resolution; ii) dynamic range that covers the total human visual range from starlight to sunlight; and iii) large field of view. Therefore, it is possible to generate an image of the sky using the Radiance software and use it as an image input in the IBL technique. Note that although the sky is the same, it is defined through a mathematical model in PBR, and in the form of an image in the IBL technique.

Radiance software uses a hybrid deterministic / stochastic (Monte Carlo) technique, where direct lighting components are computed with rays traced to random locations on the light sources (Ward, 1994; Ward and Shakespeare, 1997). In PBR approach, the sun and sky are defined as explicit light sources. Sun is explicitly defined as a source with 0.5° arc, and unobstructed sun is computed with the deterministic ray tracing algorithm: i.e. a single sample ray is sent from the camera position towards the sun and its contribution is calculated based on the known size and luminosity of sun. In IBL approach, sun and the sky are embedded within the HDR image. The image is processed through Monte Carlo ray tracing algorithm which is based on random sampling. The premise of this technique is that photons in the physical world bounce randomly, and collectively they provide stable lighting conditions (Ward, 1994). However, since the sun is not explicitly modeled as a concentrated light source, and it is calculated as part of the indirect calculation, there is a possibility that it may be overlooked in the random sampling process. Obviously, this may lead to unacceptable errors. To overcome this problem, concentrated light sources are extracted from the HDR images of the sky dome, and they are added to the simulation as direct (concentrated) light sources (Radiance *mksource* program). The concentrated light sources in this study are determined by tracing one million rays to the sky image, where the top 2 percentile of the environment is extracted as a direct light source, and the maximum source diameter is restricted to 5°. The objective of this part of the research is to investigate whether PBR and IBL approaches yield similar results.

Two sets of simulations are generated. In the first set, luminance distribution patterns are compared with the two techniques under CIE clear, intermediate and overcast skies for March 21st for 3:00 pm. Figure 8 shows the images simulated under these three sky models, where the sky models are defined with a mathematical model (PBR) and an image (IBL) generated based on the mathematical model, respectively. False color images show the error percentages for IBL images in comparison to PBR. There are minor differences between the images at the pixel level due to algorithmic differences. The average error percentages between the two algorithms are calculated as 6.8, 8.8, and 1.3% for the clear, intermediate, and overcast skies, respectively. As expected, the highest error percentage occurs under intermediate skies. In this sky model, the luminance spread across the sky dome makes it relatively difficult to identify the light sources to be calculated through the deterministic ray tracing algorithm.

In the second theoretical evaluation set, illuminance levels across a measurement grid are studied and compared with the two techniques under a CIE clear sky for June 21st at 14:00. Figure 9 demonstrates the results from this study. The illumination levels are very similar. The scatter plots demonstrate that there is high correlation (≥ 0.97) between the results.

It is important to emphasize the importance of identifying the concentrated light sources. Figure 10 demonstrates a comparison between a PBR technique, and two IBL techniques. In the first IBL model, the sky image is processed through Monte Carlo ray tracing algorithm (indirect). In the second IBL model, the top 2% of the environment is converted into explicit light sources and processed through deterministic ray tracing algorithm, and the rest of the sky dome is processed through Monte Carlo ray tracing algorithm (direct + indirect). The indirect IBL model introduces increased variations and errors compared to the PBR model and the IBL model with direct and indirect calculations.

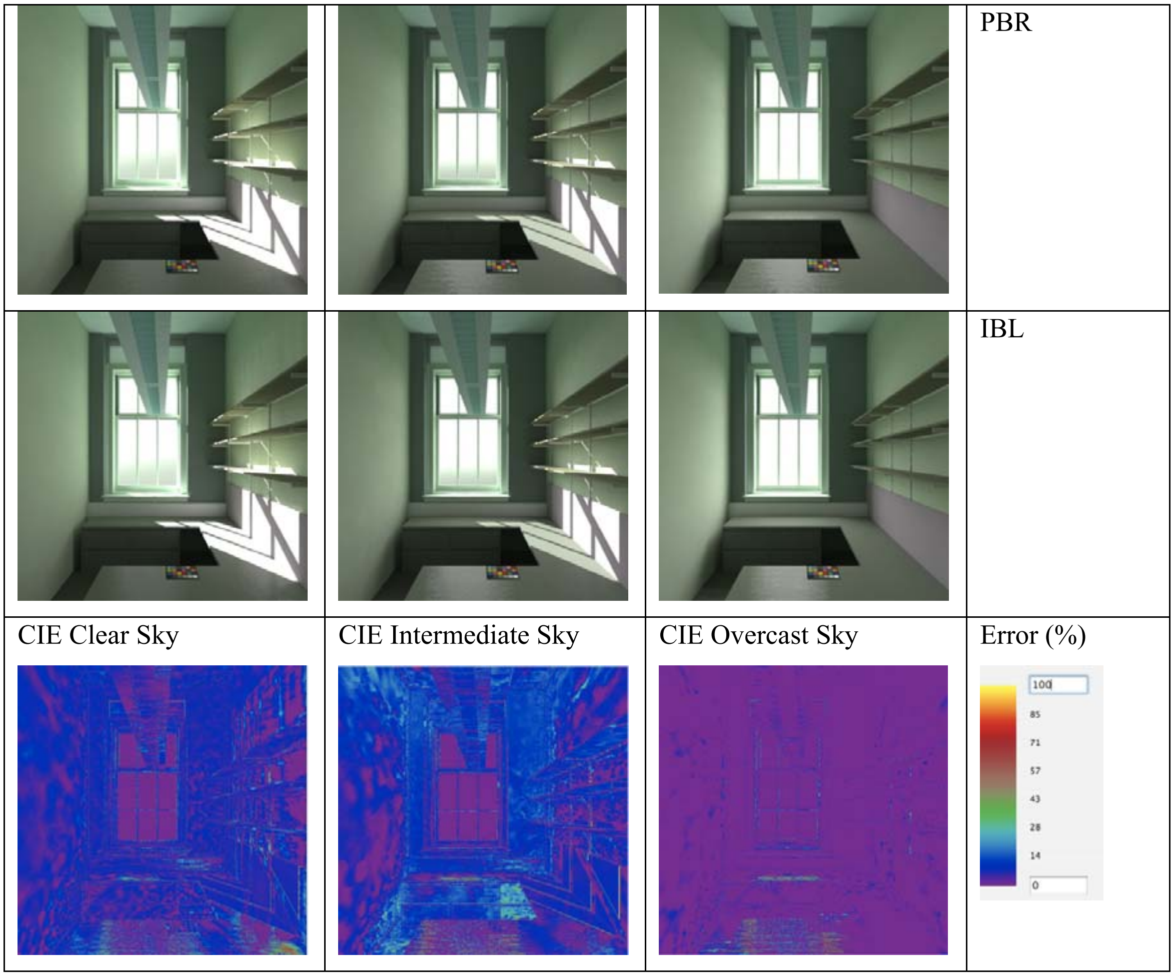

Fig. 8. Comparison of the office simulated with CIE clear, intermediate and overcast skies for March 21, 15:00: the images in the first row are generated with the mathematical model of the corresponding CIE sky (PBR), the second row images utilizes the image (IBL) of the CIE sky generated based on the mathematical model; the third row displays the error percentages when the PBR technique is compared with IBL.

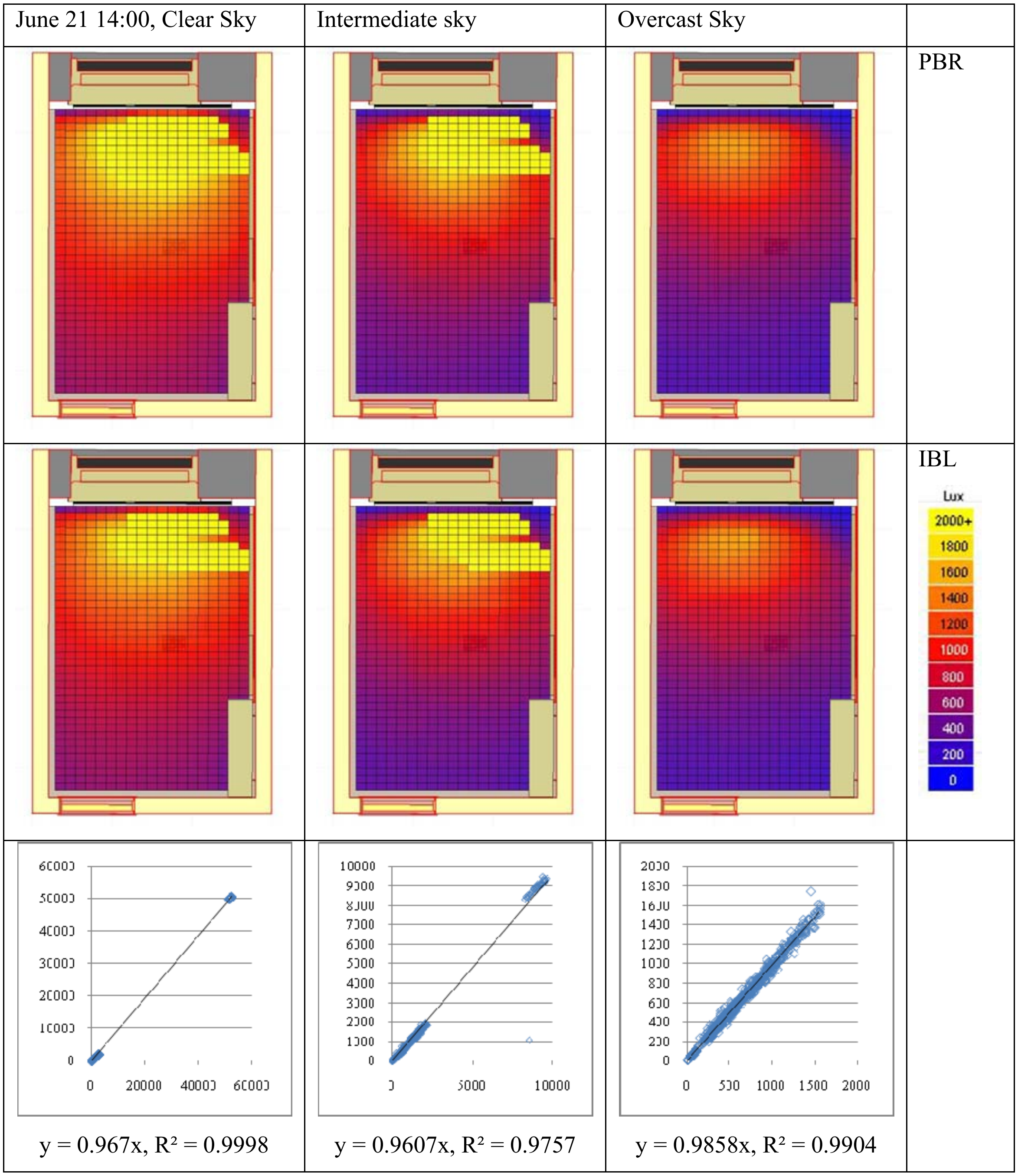

Fig. 9. Illuminance values are represented in a grid as a comparison of the same scene simulated with CIE clear, intermediate, and overcast sky models for June 21 14:00 with PBR and IBL techniques, respectively.

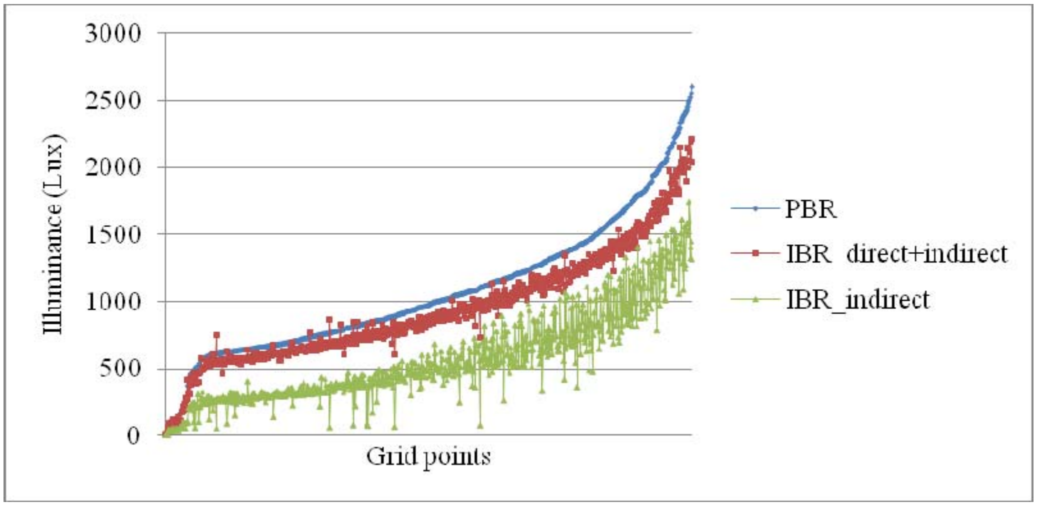

Fig. 10. Comparison of illuminance values between the PBR technique, IBL technique with indirect calculation, and IBL technique with incorporated direct and indirect calculation for June 21 14:00 under clear sky conditions

3.2 EMPIRICAL EVALUATION

For the empirical evaluation, the interior office space is simulated using the HDR images of the sky dome that were collected at the roof of the office building. Simulation results are analyzed in comparison to the HDR images of the interior office that were captured simultaneously at the same time with the sky images. Multiple data sets were collected. Four sets are presented here (Fig. 11):

- Cloudy sky (Jan 29, 14:30): The horizontal illuminance at the camera level was measured as 17,976 lux.
- Partly cloudy sky (Jan 28, 14:30): The horizontal illuminance at the camera level was measured as 24,757 lux.
- Mostly clear sky (Jan 30, 14:00): The horizontal illuminance at the camera level was measured as 34,445 lux.
- Clear sky (July 8, 14:15): The horizontal illuminance at the camera level was measured as 102,000 lux.

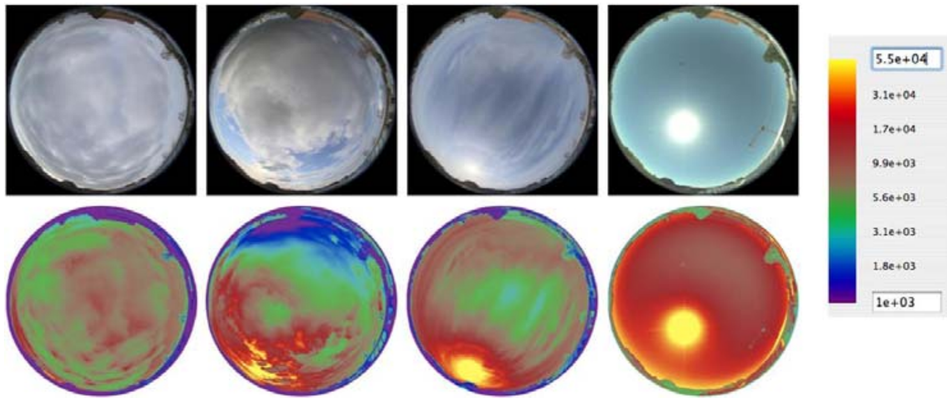

Fig. 11. Examples of captured sky images

Figure 12 demonstrates the captured HDR photograph and the simulated IBL scene with the partly cloudy sky. As seen from the scene outside the window, there are differences between the simulated and captured scenes. The sky dome was captured at the roof level and it does not include the surrounding objects that are below this level (such as the trees and low buildings seen from the office window). One of the most important advantages of using an IBL technique is that the input image, not only contains the sky, but also the surrounding structures and vegetation. Therefore, it is site specific. Neighboring structures block portions of the sky, and they reflect light based on their material properties. Although it is possible to digitally model the surrounding and include it in the simulations, there are known challenges: Modeling neighboring structures and vegetation can be computationally expensive, especially in dense urban or forestal areas. Trees are particularly difficult to model, and they filter light in a complex manner that is not straightforward to approximate. It is possible to model the surrounding buildings, but it is not a straightforward task to determine the reflectance properties of all building materials at an urban level. Depending on the site, the impact of the surrounding on lighting quantity and quality can be substantial. An HDR image captures the amount of light reflected from all of the neighboring structures towards the camera; therefore, it eliminates the need to digitally model the geometry, physically based material properties of the surrounding, and to compute the interreflections between these outside surfaces.

Fig. 12. Photograph and simulated image of the office under partly cloudy sky

Using the HDR image of the sky dome at a relatively unobstructed roof is useful for recording actual sky conditions for a wider location. For site specific sky models that can be used in simulation and analysis of un-built projects, where the building site is empty, HDR images should be taken close to the ground level to include the entire surrounding environment. For existing structures, one or more vertical fisheye images should be used to capture the sky and surrounding (Fig. 13). This method has been originally proposed by Torres (2003). To evaluate the use of IBR technique in the studied office space, vertical fisheye method has been adopted. A vertical fisheye image taken outside the window captures the sky and surrounding as seen from the interior.

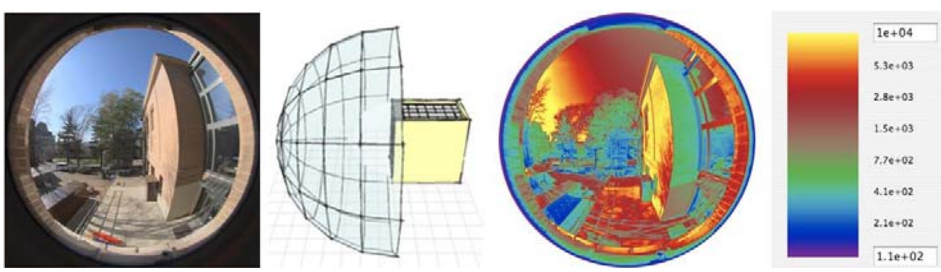

Fig. 13. Vertical fisheye image taken outside the window of the office is used as the lights source in the IBL technique to simulate the office interior

Multiple data sets were collected between December and July. Four sets are presented here:

- Cloudy sky (December, 10:00): vertical illuminance at the camera level was measured 1,496 lux.
- Partly cloudy sky (December 23, 14:00): vertical illuminance at the camera level was measured 5,220 lux.
- Clear sky (Feb 20, 13:00): vertical illuminance at the camera level was measured 7,965 lux.
- Clear sky (July 29, 16:00): vertical illuminance at the camera level was measured 63,100 lux.

Figure 14 demonstrates the false color analysis of the sky images, HDR photographs of the office interior, and the IBL simulation under the captured sky images. IBL technique incorporates the appearance of outside structures and vegetation as well as the reflected light from the surrounding, therefore, improves the accuracy of luminance predictions over the window surface and throughout the interior.

Although per-pixel comparisons can be made between the captured and simulated images, it is neither realistic nor useful to expect luminance values to match at a pixel level due to unavoidable uncertainties and simplifications in the input, measurement, and simulation processes (Rushmeier et al., 1995). It is also acknowledged that although absolute errors are not major concern for most lighting designers, relative errors can have great consequences in the design decisions (Navvab, 2003). Therefore, the comparison should focus on the spatial luminance distributions in the whole image as well as on critical task surfaces. False color luminance images of the simulated and captured office interior under different skies (Fig. 14) demonstrate that the luminance distributions are comparable. Descriptive statistic for the studies scenes are given in Table 1.

Table 1 Descriptive statistics of studied scenes

	HDR - Dec 1	IBL -Dec 10	HDR - Dec 1	IBL -Dec 14	HDR - Feb13	IBL -Feb13	HDR-July29	IBL-July29
Minimum	0.1	0.1	0.3	0.3	0.6	0.4	5.1	2.9
Maximum	1295	1351	2941	2938	4369	2011	7930	11356
Mean	22	18	58	45	125	100	333	510
Median	7	7	24	19	34	24	135	120
Std	56	38	132	90	240	172	562	842

Figure 15 provides a comparison between the HDR image of the office interior, IBL simulation of the office with sky conditions captured in July 29 at 16:00, and the PBR simulation of the office under CIE clear sky conditions, for the same date and time. An HDR image used for IBL simulation captures not only the sky luminance distributions, but also sky obstructions due to geometric composition of the surrounding structures, and the amount of reflected light from surrounding structures. Therefore, it eliminates the need to digitally model the geometry, physically based material properties of the surrounding, and to compute the interactions between these outside surfaces. This provides practicality and efficiency in modeling the impact of surrounding on simulation results.

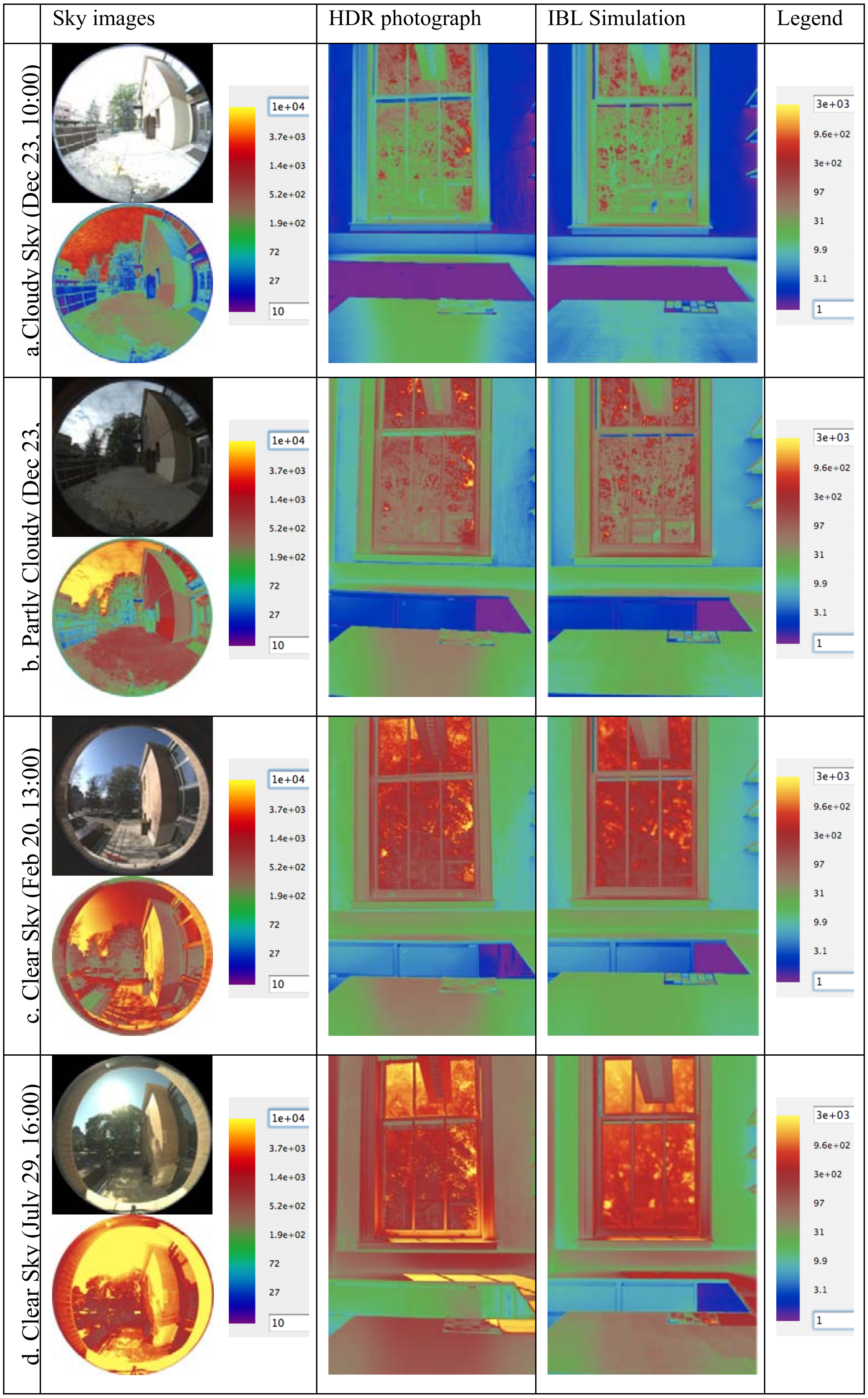

Fig. 14. False color images of the office from a) HDR photograph, b) simulation using the IBL technique and vertical fisheye image as the light source, and c) simulation using CIE clear sky as the light source

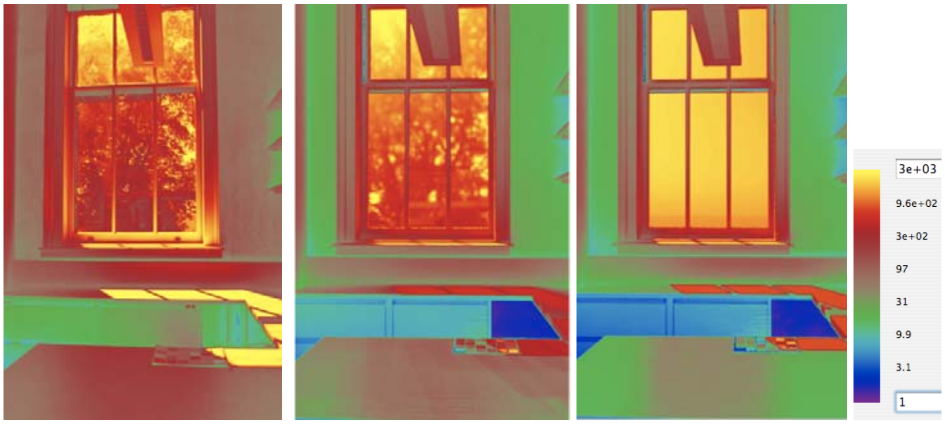

Fig. 15 Comparison of the HDR image of the sky, IBL simulation, and PBR simulation under clear sky conditions for July 29, 16:00.

4. CONCLUSION

The paper has demonstrated that image based sky models can provide an accurate and efficient method for defining the sky luminance distributions and the impact of surrounding urban fabric and vegetation as compared to generic CIE sky models and explicit modeling of surrounding urban fabric and forestry. Theoretical validation results attest that accurate results can be achieved in IBL technique with adequate lighting calculation parameters and techniques. For best simulation results, sky models can be captured at the site and close to the ground level for un-built projects. For existing structures, vertical fisheye images that capture the sky as well as the surrounding are recommended for best results. Using the HDR image of the sky dome at a relatively unobstructed roof is useful for capturing actual sky conditions occurring at a specific time, but they will lack the benefit of incorporating the impact of surrounding urban fabric and vegetation.

Increased accuracy of simulations is needed to develop better performance analysis tools, techniques, and metrics. IBL technique is particularly useful for visual comfort and performance metrics, where interior luminance ratios and accurate depiction of window luminance distributions are critical.

ACKNOWLEDGEMENT

I thank Greg Ward from Anyhere Software for his advice on various technical issues. Nan Ching Tai created the 3D model of the office space used for the simulation, and assisted during the HDR image capturing process. I thank Lawrence Berkeley National Laboratory, Building Technology Group for their generosity in lending the spectroreflectometer I used in this research. This research is funded by the University of Washington Royalty Research Fund.

5. REFERENCES

Chain C, Dumortier D, Fontoynont M. 2001. Consideration of daylight's color. Energy and Buildings. 33(3): 193-198.

[CIE] Commission International de l'Eclairage. 2003. Spatial distribution of daylight – CIE standard general sky. Vienna (Austria). CIE Publication No. S 011/E.

de Valpine J. 2006. Night Lighting Simulation: Design evaluation using Radiance's rtconrib and mksource programs. 5th International Scientific Radiance Workshop. De Montfort University, Leicester (UK). < http://www.radiance-online.org/radiance-workshop5/2006_Radiance_Workshop/Presentations/JackdeValpine.pdf> Accessed 2010 July 29.

Debevec P, Malik J. 1997. Recovering High dynamic range radiance maps from photographs. Proceedings of SIGGRAPH 97, Computer Graphics Proceedings, Annual Conference Series. Los Angeles (California): 369-378.

Debevec P. 2002. Image-based lighting. IEEE Computer Graphics and Applications. 22(2): 26-34.

Debevec P. 2005. Making the Parthenon. 6th International Symposium on Virtual Reality, Archaeology, and Cultural Heritage, Pisa (Italy).

Inanici M and Galvin J. 2005. Evaluation of High Dynamic range photography as a luminance mapping technique. LBNL Report no. 58656.

Inanici M. 2006. Evaluation of high dynamic range photography as a luminance data acquisition system. Lighting Research and Technology. 38(2):123-136.

Kitler R, Hayman S, Ruck N, Warren J. 1992. Daylight measurement data: Methods of evaluation and representation. Lighting Research and Technology. 24(4):173-187.

Navvab M. 2005. Spectral variability of daylight within luminous environment. Proceedings of the International Commission on Illumination CIE 2005 Mid-Conference, Leon, Spain.

Navvab M. 2003. Validation of algorithms for daylight outdoors and indoors. Proceedings of the International Commission on Illumination (CIE) 2003 Conference, San Diego, USA.

Reinhard E, Ward G, Pattanaik S, Debevec P. 2006. *High* Dynamic range imaging: acquisition, display, and image-based lighting. San Francisco : Morgan Kaufman Publisher. 502 p.

Rushmeier H, Ward G, Piatco C, Sanders P, Rust B. 1995. Comparing real and synthetic images: some ideas about metrics. *6th Eurographics Workshop on Rendering* Springer-Verlag, Dublin (Ireland).

Shahriar ANM, Hyde R, Hayman S. 2009. Wide-angle Image analysis for sky luminance measurement. Architectural Science Review. 52(3):211-220.

Spasojevic B, Mahdavi A. 2007. Calibrated sky luminance maps for daylight simulation applications. Proceedings of the International Building Performance and Simulation Association 2007 Conference. Beijing, China.

Stumpfel J, Jones A, Wenger A, and Debevec P. 2004. Direct HDR capture of the sun and sky. 3rd International Conference on Virtual Reality, Computer Graphics, Visualization and Interaction in Africa. Cape Town, South Africa.

Torres S. 2003. Experiences with luminance mapping for daylighting simulations. 2nd International Scientific Radiance Workshop. Berkeley, California.

Uetani Y, Navvab M, and Matsuura K. 1993. Cloud cover measurement using color video images. Proceedings of the 7th European Lighting Conference LUX EUROPA. Vol. 2: 614-621.

Ward G, Shakespeare R. 1997. Rendering with Radiance. California: Morgan Kaufman Publishers. 664 p.

Ward G. 1994. The Radiance lighting simulation and rendering system. Proceedings of SIGGRAPH 94, Computer Graphics Proceedings, Annual Conference Series. 459-572.

Ward G. 2005. Photosphere. <http://www.anyhere.com/> Accessed 2010 July 29.